Journal of Electroanalytical Chemistry 950 (2023) 117892

Contents lists available at ScienceDirect

Journal of Electroanalytical Chemistry

journal homepage: www.elsevier.com/locate/jelechem

Room temperature electro-carboxylation of styrene and stilbene derivatives: A comparative study

Nada Alhathlaul [a,b], Zeliha Ertekin [a,c], Stephen Sproules [a], Mark D. Symes [a,*]

[a] WestCHEM, School of Chemistry, University of Glasgow, G12 8QQ Glasgow, UK
[b] Chemistry Department, College of Science, Jouf University, P.O. BOX:2014, Sakaka, Saudi Arabia
[c] Hacettepe University, Faculty of Science, Department of Chemistry, Beytepe, 06800 Ankara, Turkey

ARTICLE INFO

Keywords:
Electrochemical carbon dioxide reduction
Electrocatalysis
Styrene
Stilbene
Carboxylation

ABSTRACT

The use of carbon dioxide as a comparatively cheap, abundant and non-toxic C-1 synthon is a topic of considerable interest and importance. The electrochemical addition of carbon dioxide across carbon–carbon double bonds is one of the more promising of such procedures, offering the possibility to convert a range of alkene substrates to valuable carboxylated products. However, much remains unknown about both the mechanism of reaction and how to influence product specificity during electro-carboxylation of alkenes. Herein, we explore the electrochemical addition of carbon dioxide (1 atm) to a range of olefinic substrates using nickel working electrodes and magnesium anodes at room temperature, producing the mono-substituted carboxylate derivatives preferentially (with no formation of the Markovnikov isomers of these mono-substituted carboxylate derivatives when the starting materials are non-symmetrical). These findings are rationalized using both experimental and computational methods, suggesting that the choice of Ni as a working electrode is critical in determining the reaction outcomes that are observed. Moreover, we also present direct evidence that a pathway whereby the alkene substrates are first reduced at the electrode surface and then react with dissolved CO_2 is operating. Together, these results offer the potential for selective access to a range of valuable mono-carboxylic acids via the reduction of the corresponding alkene precursors in the presence of carbon dioxide.

1. Introduction

Carbon dioxide emissions from burning fossil fuels are a major contributor to climate change, which is having increasingly serious environmental impact [1,2]. At the same time, carbon dioxide is a valuable potential building block for the production of synthetic value-added chemicals [3,4]. Electrochemical methods for the reduction of carbon dioxide (and/or its incorporation into substrate materials) are very appealing in this regard, as electrochemical technologies are inherently scalable [5,6], whilst also offering the ability to couple directly to renewable energy sources [7,8].

One avenue for employing carbon dioxide in synthesis via electrochemical means is the reduction of alkene substrates in the presence of CO_2, leading to addition of carboxylate units across the C═C bond and yielding highly desirable mono- and di-substituted carboxylic acids [9]. The exploration of this field has garnered significant attention in recent years and a selection of key reports in this area is summarized in Table 1. For example, Filardo et al. [10] studied the reduction of carbon dioxide at a graphite electrode in *N,N*-dimethylformamide (DMF) solvent containing tetrabutylammonium bromide (Bu_4NBr) as the supporting electrolyte at applied potentials between −2.15 V and −2.20 V (vs. Ag/AgI) in a tank cell and obtained a mixture of 3-phenylpropionic and phenylsuccinic acids (Table 1, entry 1). Some of the same authors subsequently explored a wider range of potentials and reported somewhat altered product distributions [11] (Table 1, entry 2).

Most studies in this area appear to have been conducted under fixed current regimes, rather than at fixed potential. In a fixed current regime, the potential is increased until the desired current is achieved. This makes the process useful in industrial electrochemical processes as a defined amount of product can be obtained in a defined time (as a function of the current and the Faradaic yield for the reaction). However, there is in general less control than with a fixed potential regime, whereby a potential is set and then only reactions that can occur at that potential will take place. Fixed potential regimes therefore may display better Faradaic efficiencies, but at the cost of increased reaction time, as the currents passing at the fixed potential may be limited. To this end,

---

* Corresponding author.
E-mail address: mark.symes@glasgow.ac.uk (M.D. Symes).

https://doi.org/10.1016/j.jelechem.2023.117892
Received 17 August 2023; Received in revised form 12 October 2023; Accepted 25 October 2023
Available online 29 October 2023
1572-6657/© 2023 The Author(s). Published by Elsevier B.V. This is an open access article under the CC BY license (http://creativecommons.org/licenses/by/4.0/).

Table 1
A selection of conditions, conversions and yields for the electro-reduction of alkenes in the presence of CO_2 from the literature.

Entry	Alkene	Reaction Conditions	Conversion	Products and Yield	Ref
1	Styrene	Working electrode: Graphite electrode Counter electrode: Aluminum electrode Medium: DMF, Bu_4NBr, and continuously bubbling CO_2Technique: Controlled potential electrolysis (−2.45 to −2.50 V vs Ag/AgI), current density 12–24 mA/cm^2 Cell type: diaphragmless tank cell Reaction temperature: Room temperature	60 %	3-phenylpropionic acid (29 %) Phenylsuccinic acid (60 %)	[10]
2	Styrene	Working electrode: Graphite electrode Counter electrode: Aluminum electrode Medium: DMF, Bu_4NI, and continuously bubbling CO_2Technique: Controlled potential electrolysis (−2.7 V vs Ag/AgI). Cell type: diaphragmless tank cell Reaction temperature: Room temperature	87 %	Phenylsuccinic acid (40 %)Phenylpropionic acid (35 %)3,4-diphenyladipic acid (10 %)	[12]
3	Styrene	Working electrode: Carbon fiber electrode Counter electrode: Magnesium electrode Medium: DMF, tetrabutylammonium tetrafluoroborate, CO_2 (1 atm) Technique: Current 50 mA, 5–7 h Cell type: single-compartment cell Reaction temperature: 20 °C Catalyst: Ni complexes with several pentamethyl diethylene triamines	40 %	Phenylsuccinic acid (85 %)	[13]
	α-Methyl Styrene		35 %	2,2-Disubstituted Succinic acid (71 %)	
	E-β-Methyl Styrene		45 %	Mono and Dicarboxylic acids (44 %)	
	1,1-Diphenylethylene		25 %	2,2-Disubstituted Succinic acid (95 %)	
4	Styrene	Working electrode: Platinum plate Counter electrode: Magnesium rod Medium: DMF, tetraethylammonium perchlorate, CO_2 (1 atm) Technique: Constant current electrolysis (25 mA/cm^2) Cell type: 2-Compartment cell Reaction temperature: −10 °C Styrene was electrolyzed in the presence of 4-methoxyphenol.	73 %	Phenylsuccinic acid (66 %)	[14]
	α-Methyl Styrene		98 %	2,2-Disubstituted succinic acids (68 %)	
	E-β-Methyl Styrene		98 %	2-Methyl-3-phenylsuccinic acid (77 %)	
	Z-β-Methyl Styrene		98 %	2-Methyl-3-phenylsuccinic acid (70 %)	
	1,1-Diphenylethylene		93 %	2,2-Disubstituted succinic acids (91 %)	
	E-Stilbene		84 %	2,3-Diphenylsuccinic acid (84 %)	
	Z-Stilbene		84 %	2,3-Diphenylsuccinic acid (84 %)	
5	Styrene	Working electrode: Nickel plate Counter electrode: Zinc plate Medium: DMF, n-Bu_4NBr, and CO_2 4 MPa.Technique: Constant current (10 mA/cm^2), two electrode set-up Cell type: high-pressure stainless-steel undivided cell Reaction temperature: Room temperature.	–	Phenyl succinic acid (50 %)	[15]
		Working electrode: Nickel plate Counter electrode: Magnesium plate Medium: DMF, n-Bu_4NBr, and CO_2 4 MPa.Technique: Constant current (10 mA/cm^2), two electrode set-up Cell type: high-pressure stainless-steel undivided cell Reaction temperature: Room temperature.	–	Phenyl succinic acid (85 %)	
		Working electrode: Nickel plate Counter electrode: Aluminum plate Medium: DMF, n-Bu_4NBr, and CO_2 4 MPa.Technique: Constant current (10 mA/cm^2), two electrode set-up Cell type: high-pressure stainless-steel undivided cell Reaction temperature: Room temperature.	–	Phenyl succinic acid (87 %)	
		Working electrode: Platinum plate Counter electrode: Aluminum plate Medium: DMF, n-Bu_4NBr, and CO_2 4 MPa.Technique: Constant current (10 mA/cm^2), two electrode set-up Cell type: high-pressure stainless-steel undivided cell Reaction temperature: Room temperature.	–	Phenyl succinic acid (89 %)	
	α-Methyl Styrene	Working electrode: Nickel plate Counter electrode: Aluminum plate Medium: DMF, n-Bu_4NBr, and CO_2 4 MPa.Technique: Constant current (10 mA/cm^2), two electrode set-up Cell type: high-pressure stainless-steel undivided cell Reaction temperature: Room temperature.	–	2-Methyl-2-phenyl succinic acid (85 %)	
6	Styrene	Working electrode: Copper electrode Counter electrode: Carbon electrode Medium: DMF, n-Bu_4NI (0.04 M), triethylamine (0.04 M); triethanolamine (0.04 M), CO_2 (1 atm). Technique: Constant current at 60 mA, 24 h Cell type: undivided cell, two-electrode set-up (5–10 V typically applied) Reaction temperature: 50 °C	99 %	3-Phenylpropanoic acid: 4-phenyl-1,3-dioxolan-2-one(3:1) ratio Phenylsuccinic acid: 3-phenylbutanoic acid(5:1) .	[16]
		Working electrode: Copper electrode Counter electrode: Aluminum electrode Medium: DMF, n-Bu_4NI (0.04 M), and CO_2 (1 atm). Technique: Constant current at 60 mA, for 24 h Cell type: undivided cell, two-electrode set-up (5–10 V typically applied) Reaction temperature: 50 °C	–	2-phenylbutanoic acid (68 %)	

(continued on next page)

Table 1 (*continued*)

Entry	Alkene	Reaction Conditions	Conversion	Products and Yield	Ref
7	Styrene	Working electrode: Nickel Mesh Counter electrode: Magnesium rod Medium: DMF, $n\mathrm{Bu_4NPF_6}$, and CO_2 (continuously supplied)Technique: Constant current electrolysis (35 mA) for 8 h Cell type: undivided cell Reaction temperature: Room temperature.	80 %	Phenylsuccinic acid (13 %); 3-Phenylpropionic acid (53 %)	This work
	α-Methyl Styrene		72 %	3-Phenylbutyric acid (68 %)	
	E-β-Methyl Styrene		79 %	2-Methyl-3-phenylpropionic acid (69 %)	
	Z-β-Methyl Styrene		78 %	2-Methyl-3-phenylpropionic acid (68 %)	
	1,1-Diphenylethylene		75 %	2,3-Diphenylsuccinic acid (50 %)	
	E-Stilbene		74 %	2,3-Diphenylsuccinic acid (10 %); 2,3-Diphenylpropionic acid (47 %)	
	Z-Stilbene		84 %	2,3-Diphenylsuccinic acid (18 %); 2,3-Diphenylpropionic acid (44 %)	

Dérien et al. explored the use of Ni complexes as homogeneous catalysts for the electrochemically-driven addition of CO_2 to alkenes (Table 1, entry 3) at a fixed current of 50 mA, again using a carbon-based working electrode [12]. A range of substrates were tested (styrene, α-methyl styrene, E-β-methyl styrene and 1,1-diphenylethylene) and in some cases excellent yields of the substituted products were obtained.

Senboku and co-workers (Table 1, entry 4) examined a wider range of substrates still, and also replaced the carbon working electrode with a metal one (in their case, Pt). Their conditions led to a significant improvement in the conversion of the alkene substrates (essentially complete conversion in many cases), whilst still maintaining good-to-excellent yields for the functionalized substrates [13].

In 2008, Yuan et al. investigated the electrosynthesis of 2-aryl succinic acids by reacting carbon dioxide with a variety of aryl-substituted alkenes in an undivided electrochemical cell. These authors also employed their CO_2 at pressures above atmospheric (4 MPa) and comparatively modest current density (10 mA/cm^2). Of particular note, the authors compared the effect of using a Pt working electrode with using an Ni working electrode, and were able to prepare the 2-aryl succinic products in fair to good yields (50–87 %) with high selectivity (Table 1, entry 5) [14].

More recently, Alkayal et al. have studied the effect of using non-sacrificial counter electrodes during the electrolysis. In the vast majority of studies, a sacrificial anode is used, usually magnesium, such that Mg^{2+} ions are released into solution during the electrolysis which then bind to the acid products as they form. Alkayal et al. studied the use of copper working electrodes with both aluminium and carbon anodes at 50 °C in an undivided cell and developed a highly regioselective process for the formation of β-hydrocarboxylated products from substituted alkene substrates with potentially considerable synthetic utility (Table 1, entry 6) [15].

Inspired by these earlier studies, herein we report a study on the electrochemically-driven addition of CO_2 to a range of alkene substrates at nickel working electrodes at room temperature (20 °C) and under 1 atm of carbon dioxide in a simple undivided cell in DMF, using the electrochemically inert electrolyte tetrabutylammonium hexafluorophosphate ($n\mathrm{Bu_4NPF_6}$). Our results show that there is still much that remains unknown about the process(es) by which CO_2 adds to alkenes under such electrochemical conditions, and that much remains to be optimized. Of particular note, we show a bias in favor of forming mono-substituted acid products, where the carbon dioxide adds exclusively to the position β to the aromatic ring in the substrates we examine, possibly as a result of using an Ni working electrode. We also provide direct evidence that the pathway whereby the alkenes are reduced at the electrode surface and then react with dissolved CO_2 is operating, adding credence to some of the mechanisms previously proposed for this class of reaction.

2. Experimental section

2.1. Materials

Materials that are readily available for purchase (including supporting electrolytes, solvents, and alkenes) were used without undergoing any additional purification steps. Styrene (99 % purity), α-methyl styrene (99 % purity), *trans*-β-methyl styrene (97 % purity), *cis*-β-methyl styrene (>98 % purity), 1,1-diphenylethylene (98 % purity), *trans*-stilbene (98 % purity) and *cis*-stilbene (97 % purity) were purchased from commercial sources and used as received. All the alkenes used in this study were purchased from Alfa Aesar, with the exception of Z-β-methyl styrene which was procured from TCI. The solvent used in this study, *N,N*-dimethylformamide, anhydrous, 99.8 % purity, was obtained from Alfa Aesar and packaged under Argon. The supporting electrolyte, tetrabutylammonium hexafluorophosphate ($n\mathrm{Bu_4NPF_6}$, 98 % purity) at a concentration of 0.1 M, was purchased from ThermoFisher Scientific. Carbon dioxide, with a purity of 99 %, was purchased from BOC Ltd.

2.2. Electrochemical procedures

A BioLogic SP-150 potentiostat was employed for all cyclic voltammetry and chronopotentiometry experiments. The electrochemical carboxylation of the alkenes was conducted using a one-compartment electrochemical cell with five necks (see Fig. 1). The electrodes were situated in three of these necks, while the remaining two were designated for the gas inlet and outlet channels. The reference electrode utilized was a saturated calomel electrode (CHI150, supplied by IJ Cambria Scientific Ltd), and the counter electrode (anode) was a magnesium rod measuring 6.35 mm in diameter and 25.4 mm in length, at a purity of 99.95 % (metal basis) from Alfa Aesar. A nickel disc (BASi, 3.0 mm diameter) or a nickel mesh (0.35 × 2 cm^2, woven wire, 60 mesh, made from 0.18 mm wire, supplied by Alfa Aesar) were used as the working electrodes for cyclic voltammetry and bulk electrolysis respectively.

Prior to bulk electrolysis, the Ni mesh was sonicated in a sonication bath in 2 M HCl for 20 min and then rinsed with DMF. Meanwhile, the magnesium rod was sonicated in a sonication bath in DMF for 20 min. Both electrodes were then allowed to dry in the air. Bulk electrolysis was then initiated at room temperature (20 °C) with stirring under a constant stream of CO_2. In all cases, the electrolyte consisted of 0.1 M $n\mathrm{Bu_4NPF_6}$ in anhydrous *N,N*-dimethylformamide (volume = 20 mL). Into this volume of electrolyte, 3.5 mmol of alkene substrate was dissolved, giving a concentration of alkene substrate in the electrolyte of 0.175 M. For all bulk electrolyses, a fixed current of −35 mA was applied to the working electrode for 8 h (corresponding to the passage of 3*F* of charge relative to the number of moles of

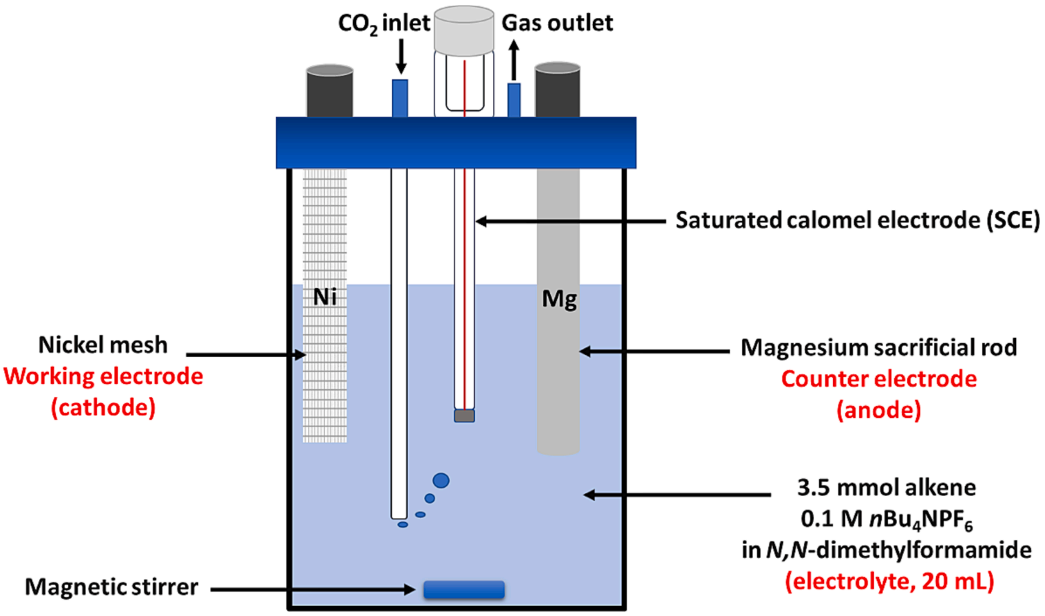

Fig. 1. An illustration of the cell set-up for both cyclic voltammetry and bulk electrolysis in this study.

alkene present). The voltage required to deliver such currents was typically within the range −3 to −5.5 V vs SCE.

All cyclic voltammetry was performed under the same conditions and in the same cell as for bulk electrolysis, except using a Ni disc button working electrode (BASi, 3 mm diameter). Cyclic voltammograms were recorded under Ar and under CO_2 for comparison (in both cases after bubbling for 20 min). The working electrode was polished between experiments. Cyclic voltammetry was recorded at a scan rate of 10 mV/s over the range 0 V to −3 V vs. SCE, starting from 0 V.

2.3. Workup procedure

The following procedure was adopted after bulk electrolysis for all the alkenes investigated. Firstly, the resulting electrolyte solution was placed in a round-bottomed flask, and the electrochemical cell and electrodes were washed with DMF and these rinsings added to the round-bottomed flask. The solvent was then removed under vacuum using a rotary evaporator. To the resulting residue was added 10 mL of 2.0 M hydrochloric acid (HCl) and the mixture stirred at room temperature for a duration of 3 h. The purpose of this step was to fully protonate any carboxylic acids present, in order to facilitate their extraction into organic media. In the case of α-methyl styrene, *cis*-β-methyl styrene, and *cis*-stilbene, it was found that sonication for 30 min in an ice-filled sonication bath aided with breaking up the residue after addition of the HCl. After sonication, these mixtures were then stirred at room temperature for a duration of 3 h as above. In all cases, the resulting mixture was then subjected to three successive extractions using diethyl ether, each with a volume of ether of 20 mL. It was found that chilling the aqueous phase prior to extraction was beneficial for improving the yield of products in the organic phase. The combined diethyl ether fractions were then combined and subjected to washing with saturated sodium chloride (brine solution). The organic phase was then dried using magnesium sulfate, filtered through filter paper, and evaporated using a rotary evaporator. Finally, the resulting solution was analyzed

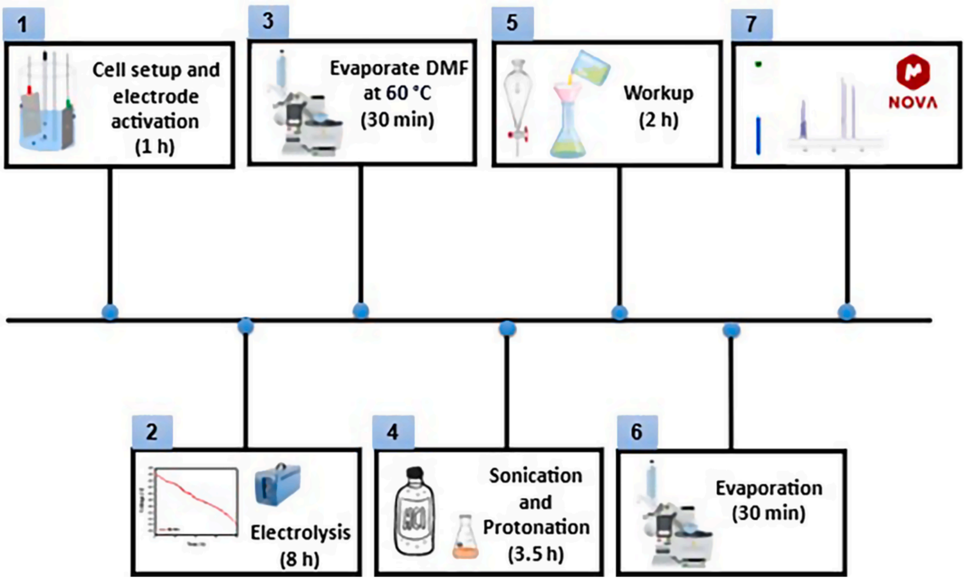

Fig. 2. An illustration of the extraction and analysis procedure used to isolate the products of electrolysis in this study.

using nuclear magnetic resonance (NMR) spectroscopy. NMR spectra were recorded at room temperature using a Bruker 400 MHz NMR spectrometer. The products were dissolved in $CDCl_3$ for analysis. The analysis procedure is summarized in Fig. 2.

2.4. Computational details

The program package ORCA was used for density functional theory (DFT) calculations [16]. Geometry optimization employed the hybrid *meta*-generalized gradient approximation M06-2X functional [17]. The def2-TZVP basis set was used for all atoms [18,19]. Auxiliary basis sets used to expand the electron density in the calculations were chosen to match the orbital basis. The RIJCOSX algorithm was used to speed the calculation of Hartree–Fock exchange [20,21]. Solvation was incorporated using the Conductor-like Polarizable Continuum Model (C-PCM) with infinite continuum [22]. The self-consistent field calculations were tightly converged (1×10^{-8} E_h in energy, 1×10^{-7} E_h in the charge density, and 1×10^{-7} in the maximum element of the DIIS [23,24] error vector). The geometry was converged with the following convergence criteria: change in energy $< 10^{-5}$ E_h, average force $< 5 \times 10^{-4}$ E_h Bohr^{-1}, and the maximum force 10^{-4} Eh Bohr^{-1}. The geometry search for all complexes was carried out in redundant internal coordinates without imposing geometry constraints. Molecular orbitals and charge density maps were visualized via the program Molekel [25].

2.5. Physical characterisation

X-ray diffraction (XRD) analysis was performed using a Rigaku Mini Flex instrument with CuKα radiation. The scanning diffraction angle 2θ range was from 5° to 80° at a speed of 5° per minute. The morphology of the nickel mesh electrodes was analyzed using a Zeiss Sigma variable-pressure field-emission scanning electron microscope (FESEM) in the Geoanalytical Electron Microscopy and Spectroscopy (GEMS) facility at the School of Geographical and Earth Sciences, University of Glasgow. The untreated and treated Ni samples were placed on sample holders and a gold layer was applied for SEM imaging, while a carbon coating was utilized for EDX analysis to enhance electrical conductivity.

3. Results and discussion

Table 2 shows conversions, isolated yields and Faradaic efficiencies for the production of various carboxylic acids from their parent alkenes under the conditions given in the experimental section, with the corresponding NMR, mass spectrometry and infrared spectroscopy data for all resulting products given in the Supporting Information (Figs. S1–S28 and Table S1). Example chronopotentiometry data for these reductions is shown in the Supporting Information as Figs. S29–S35, and details on how the yields, conversions and Faradaic efficiencies were calculated is given in Section 7 of the Supporting Information. In all cases, substrate conversion is good-to-excellent, indicating that the alkene starting materials are largely consumed during the reaction. Analysis of the Ni mesh working electrodes before and after reaction by X-ray diffraction and SEM/EDX (see Figs. S36 and S37) indicates that the cathode becomes somewhat rougher during reaction but that its composition remains essentially unchanged during the electro-reduction process (remaining as nickel metal).

However, in comparison to previous studies on electro-reduction of alkenes in the presence of carbon dioxide, the yields of mono-carboxylic acids are significantly higher and the yields of the di-carboxylic acids are correspondingly lower. For example, Senboku et al. (Table 1, entry 4) obtained yields of the dicarboxylic acids of between 65 and 91 % when operating at 263 K on a Pt cathode, with mono-carboxylic acids observed only in small amounts. Meanwhile, Yuan et al. (Table 1, entry 5) found that dicarboxylic acids predominantly formed on Ni working electrodes [14], but these authors used considerably higher pressures of CO_2 than we employed (4 MPa vs. 1 MPa). In our study, this trend for dicarboxylated products is reversed. Campbell and Young have shown that Ni cathodes (such as were used here) are capable of hydrogenating activated double bonds to a much greater extent than cadmium, lead, amalgamated lead, copper or platinum cathodes [26]. This might explain the greater propensity towards the production of mono-carboxylic acids (where hydrogen has been added in preference to a second carbon dioxide molecule) compared to analogous studies on Pt cathodes [13].

In terms of the mono-carboxylic acids that are produced, it is striking that when non-symmetrical alkene substrates are employed, the mono-carboxylic acids that are observed are all the anti-Markovnikov products (i.e. the carbon dioxide is found to add to the lesser-substituted of the two possible carbons from the alkene). The alternative arrangement (where CO_2 has added only to the more substituted carbon) is never observed. Fig. 3 illustrates the three possible products that can be formed when carbon dioxide adds to a non-symmetrical substrate such as styrene. If carbon dioxide adds at both positions of the double bond, then phenylsuccinic acid results. Conversely, if only mono-substitution occurs, then there are two possibilities for the products: 3-phenylpropionic acid (where the carbon dioxide adds to the terminal (β) position of the double bond, on the least substituted carbon) or 2-phenylpropionic acid (where the carbon dioxide adds to the more substituted (α) carbon).

To investigate this apparent regioselectivity further, density function theory (DFT) calculations were performed on all the alkene substrates in Table 2, in order to examine this preference for carbon dioxide to add at the less-substituted β-position relative to the aromatic ring (see Tables S2–S17 and Figs. S38–S51 in the Supporting Information). These data show the position of the charge density when the alkene substrates in Table 2 are reduced by one electron to give the radical anions (see Fig. 4 for possible mechanisms). In all cases, the reactive unpaired electron on the radical anions is found at the β-carbon position. This appears to be a consequence of the aromatic ring syphoning electron density off the α-carbon through conjugation, leaving the more distant β-carbon with the larger electron density. The upshot is that carboxylate substitution at the β-carbon is preferred to substitution at the α-position for all the substrates that were examined (see Supporting Information, Table S18).

Previous studies on the electro-reductive addition of CO_2 to alkenes have proposed that both pathways shown in Fig. 4 are possible, on account of the CO_2 and alkene reduction potentials being close to one another. Figs. S52–S58 (Supporting Information) show that under the conditions used in this study, direct reduction of carbon dioxide at the electrode surface does indeed occur at approximately the same position as alkene reduction, implying that both pathways could operate in our case, at least in theory. However, to the best of our knowledge, direct evidence for either pathway has yet to be observed during the electro-reductive addition of CO_2 to alkenes.

The cyclic voltammograms of *trans*-stilbene and *cis*-stilbene in the presence and absence of CO_2 are instructive in this regard (Fig. 5 and Fig. S58 respectively). Fig. 5 (black line) shows the cyclic voltammogram of electrolyte saturated with CO_2, while the red line shows the cyclic voltammogram of electrolyte with 3.5 mmol *trans*-stilbene under argon. In the latter case, a quasi-reversible redox wave centered at around −2.3 V vs. SCE is evident for the *trans*-stilbene. The blue line then shows the effect of having both CO_2 and *trans*-stilbene present: the cyclic voltammogram very much resembles that of *trans*-stilbene in argon, but it now takes on features of a catalytic wave, with enhanced reductive current and a complete absence of any return oxidation wave for the redox event centered at −2.3 V vs. SCE. This implies that the reduced *trans*-stilbene is reacting with dissolved CO_2 chemically before it can be re-oxidized electrochemically at the electrode. This in turn suggests that a mechanism whereby the alkene is initially reduced at the electrode surface (with this then going on to react with carbon dioxide) is operating (Pathway 2 in Fig. 4). Whilst these data do not exclude the possibility that Pathway 1 is operating simultaneously, they do at least

Table 2
Conversions, isolated yields, and Faradaic efficiencies for the production of various carboxylic acids.

Entry	Substrate	Substrate conversion (%)	Product	Isolated yield (%)	Faradic efficiency (%)
1	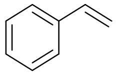	80	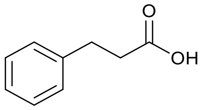	53	36
			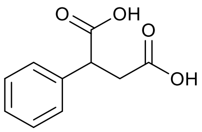	13	8
2	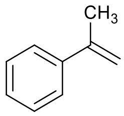	72	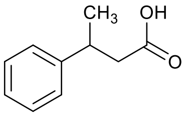	68	46
3	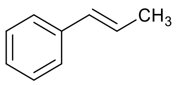	79	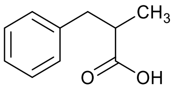	69	46
4	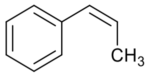	78	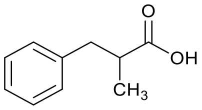	68	46
5	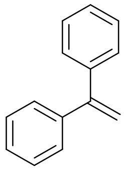	75	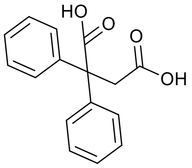	50	33
6	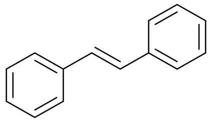	74	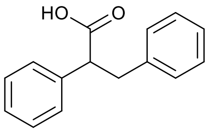	47	31
			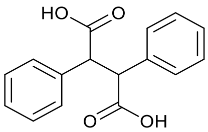	10	7
7	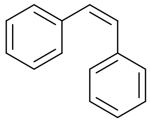	84	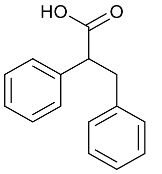	44	30

(continued on next page)

Table 2 (*continued*)

Entry	Substrate	Substrate conversion (%)	Product	Isolated yield (%)	Faradic efficiency (%)
			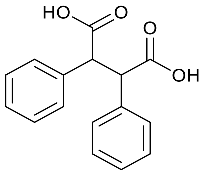	18	12

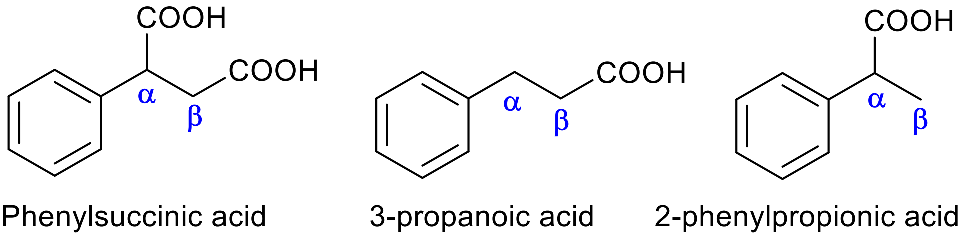

Fig. 3. The three possible structures that are possible after carboxylation of styrene.

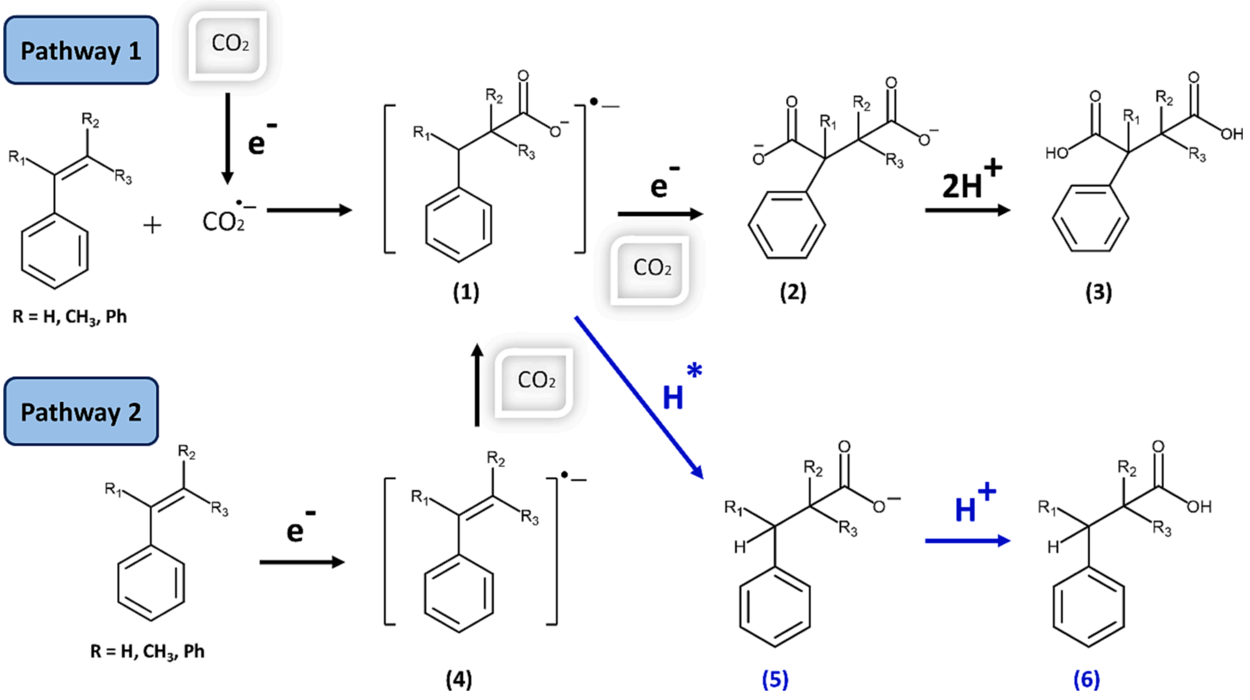

Fig. 4. The two suggested pathways for the electrochemically-driven addition of CO_2 to alkene substrates: initial CO_2 reduction at the electrode, followed by addition (Pathway 1) and initial reduction of the alkene at the electrode, followed by reaction with CO_2 (Pathway 2). Arrows in black show the proposed route to the di-carboxylic acids; arrows in blue show the proposed route to the mono-carboxylic acids.

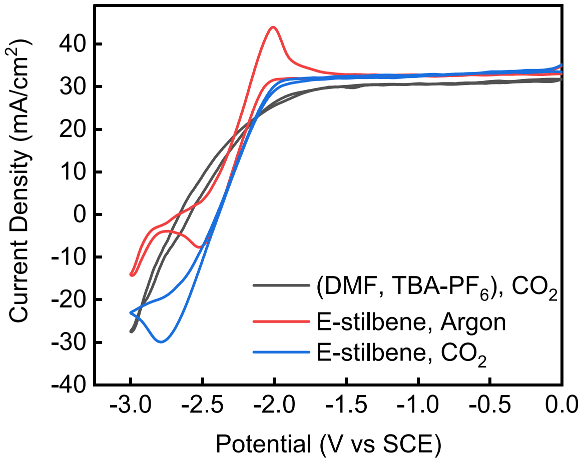

Fig. 5. Cyclic voltammetry of a 3.5 mmol solution of *trans*-stilbene in 20 mL DMF containing 0.1 M nBu_4NPF_6 supporting electrolyte at room temperature, with scan rate of 10 mV/s. A Ni disc button (3 mm diameter) was used as the working electrode, a Mg rod was used as the counter electrode and an SCE electrode was used as the reference. Color code: electrolyte saturated with CO_2 (black line), electrolyte plus 3.5 mmol of *trans*-stilbene saturated with Ar (red line), electrolyte plus 3.5 mmol of *trans*-stilbene saturated with CO_2 (blue line).

provide evidence for the occurrence of Pathway 2, demonstrating directly for the first time that the “alkene first” route is a contributor in the electro-reductive addition of CO_2 to alkenes.

These results allow a possible mechanism for the production of the mono-carboxylated species to be proposed and rationalized (see also Fig. 4). Firstly, the data in Fig. 5 show that initial reduction of the alkene occurs at the electrode surface to yield the radical anion (**4**). This radical anion then reacts with dissolved CO_2 to give the mono-carboxylated radical species (**1**). Species (**1**) can also possibly form via initial reduction of CO_2 at the electrode to give the radical anion, followed by addition of this to the neutral alkene substrate (the data do not rule this pathway out, they only show that the pathway via radical anion (**4**) is definitely operating). In any case, DFT studies suggest that this first carboxylation occurs at the position β to the phenyl ring for those substrates where the α and β labels have meaning. This would then leave a radical located at the α carbon of (**1**), which could either react with a further electron and carbon dioxide molecule (giving the dicarboxylate, (**2**)) or with putative H* on the surface of the Ni electrode (giving monocarboxylate (**5**)). By analogy with the work of Campbell and Young on electrochemical hydrogenation of double bonds at Ni electrodes [26], we postulate that H atoms adsorbed on the electrode surface add to species (**1**) in competition with the addition of a second molecule of CO_2, producing anion (**5**) in one step from species (**1**) (blue arrows in Fig. 4). Protonation of species 2 and 5 during work-up then lead to the carboxylic acid products (**3**) and (**6**) respectively.

4. Conclusions

Herein, we have studied the electro-carboxylation of a range of alkenes under 1 atm of CO_2 at 20 °C in DMF solution at a Ni working electrode. Our results present a departure from the prevailing literature in that most previous reports find that the di-carboxylic acids are by far the dominant reaction products, whereas our data show that the mono-carboxylates are formed preferentially in most cases. Through analysis of the energetics of the reaction by DFT, and by analysis of cyclic voltammograms of the substrates in the presence and absence of CO_2, we show that the addition of the first carbon dioxide molecule to the alkene occurs at the site β to the phenyl ring when this is available, and that a mechanism where the alkene is first reduced at the electrode and then reacts with CO_2 is operating (although the simultaneous operation of a competing pathway whereby the CO_2 is reduced first and then this reacts with the neutral alkene cannot be excluded). Both mono- and di-carboxylic acids can then be produced, but with a preference for the mono-carboxylates in this work, a feature that comparison with the literature suggests is due to the choice of Ni as the working electrode, which is an effective material for electrochemical hydrogenations. Overall, these results offer the prospect that this system could be further developed to allow valuable mono-carboxylate products to be produced by the electro-carboxylation of the corresponding alkene precursors with high regio-selectivity.

CRediT authorship contribution statement

Nada Alhathlaul: Methodology, Data curation, Investigation. **Zeliha Ertekin:** Investigation.**Stephen Sproules:** Investigation, Writing – review & editing. **Mark D. Symes:** Conceptualization, Supervision, Writing – review & editing.

Declaration of Competing Interest

The authors declare that they have no known competing financial interests or personal relationships that could have appeared to influence the work reported in this paper.

Data availability

The data underpinning this study have been deposited in the University of Glasgow’s Enlighten database under accession code https://doi.org/10.5525/gla.researchdata.1520.

Acknowledgments

This work was supported by the EPSRC (EP/W033135/1). NA thanks her sponsors (Jouf University, the Royal Embassy of Saudi Arabia Cultural Bureau, and the Ministry of Education in Saudi Arabia) for their financial support. ZE thanks the Scientific and Technological Research Council of Turkey (grant number: TUBITAK 2219) for a postdoctoral fellowship. MDS thanks the Royal Society for a University Research Fellowship (URF\R\211007).

Appendix A. Supplementary data

Supplementary data to this article can be found online at https://doi.org/10.1016/j.jelechem.2023.117892.

References

[1] M. Jitaru, Electrochemical carbon dioxide reduction - fundamental and applied topics (review), J. Chem. Technol. Metall. 42 (4) (2007) 333–344.

[2] M.G. Kibria, J.P. Edwards, C.M. Gabardo, C.T. Dinh, A. Seifitokaldani, D. Sinton, E. H. Sargent, Electrochemical CO2 reduction into chemical feedstocks: from mechanistic electrocatalysis models to system design, Advanced Materials. 31 (31) (2019) 1807166.

[3] Q.W. Song, Z.H. Zhou, L.N. He, Efficient, selective and sustainable catalysis of carbon dioxide, Green Chem. 19 (16) (2017) 3707–3728.

[4] J. Wang, H.Y. Tan, Y. Zhu, H. Chu, H.M. Chen, Linking the dynamic chemical state of catalysts with the product profile of electrocatalytic CO2 reduction, Angew. Chem. 133 (32) (2021) 17394–17407.

[5] M. Yan, Y. Kawamata, P.S. Baran, Synthetic organic electrochemical methods since 2000: on the verge of a renaissance, Chem. Rev. 117 (21) (2017) 13230–13319.

[6] A. Wagner, C.D. Sahm, E. Reisner, Towards molecular understanding of local chemical environment effects in electro-and photocatalytic CO2 reduction, Nat. Catal. 3 (10) (2020) 775–786.

[7] S.P.S. Badwal, S.S. Giddey, C. Munnings, A.I. Bhatt, A.F. Hollenkamp, Emerging electrochemical energy conversion and storage technologies, Front. Chem 2 (2014) 1–28.

[8] H.L. Dickinson, M.D. Symes, Recent progress in CO2 reduction using bimetallic electrodes containing copper, Electrochem. Commun. 135 (2022), 107212.

[9] a) C.K. Ran, H.Z. Xiao, L.L. Liao, T. Ju, W. Zhang, D.G. Yu, Progress and challenges in dicarboxylation with CO2, Natl. Sci. Open 2 (2) (2023) 20220024;
b) X.-F. Liu, K. Zhang, L. Tao, X.-B. Lu, W.-Z. Zhang, Recent advances in electrochemical carboxylation reactions using carbon dioxide, Green Chem. Eng. 3 (2022) 125–20220137;

c) H. Senboku, A. Katayama, Electrochemical carboxylation with carbon dioxide, Curr. Opin. Green Sus. Chem. 3 (2017) 50–54;
d) N. Salehi, B. Azizi, Electrochemical double carboxylation of unsaturated C-C bonds with carbon dioxide: an overview, J. Chem. Lett. 2 (2021) 2–8.

[10] G. Filardo, S. Gambino, G. Silvestri, A. Gennaro, E. Vianello, Electrocarboxylation of styrene through homogeneous redox catalysis, J. Electroanal. Chem. Interfacial Electrochem. 177 (1–2) (1984) 303–309.

[11] S. Gambino, A. Gennaro, G. Filardo, G. Silvestri, E. Vianello, Electrochemical carboxylation of styrene, J. Electrochem. Soc. 134 (9) (1987) 2172–2175.

[12] S. Dérien, J.C. Clinet, E. Duñach, J. Périchon, Electrochemical incorporation of carbon dioxide into alkenes by nickel complexes, Tetrahedron. 48 (25) (1992) 5235–5248.

[13] H. Senboku, H. Komatsu, Y. Fujimura, M. Tokuda, Efficient electrochemical dicarboxylation of phenyl-substituted alkenes: synthesis of 1-phenylalkane-1, 2-dicarboxylic acids, Synlett. 2001 (03) (2001) 0418–0420.

[14] G.Q. Yuan, H.F. Jiang, C. Lin, S.J. Liao, Efficient electrochemical synthesis of 2-arylsuccinic acids from CO2 and aryl-substituted alkenes with nickel as the cathode, Electrochim. Acta. 53 (5) (2008) 2170–2176.

[15] A. Alkayal, V. Tabas, S. Montanaro, I.A. Wright, A.V. Malkov, B.R. Buckley, Harnessing applied potential: selective β-hydrocarboxylation of substituted olefins, J. Am. Chem. Soc. 142 (4) (2020) 1780–1785.

[16] F. Neese, Software update: the ORCA program system, version 4.0. *Wiley Interdisciplinary Reviews: Computational Molecular*, Science 8 (1), e1327 (2018).

[17] Y. Zhao, D.G. Truhlar, Construction of a generalized gradient approximation by restoring the density-gradient expansion and enforcing a tight lieb-oxford bound, J. Chem. Phys. 128 (18) (2008).

[18] F. Weigend, R. Ahlrichs, Balanced basis sets of split valence, triple zeta valence and quadruple zeta valence quality for H to Rn: design and assessment of accuracy, Phys. Chem. Chem. Phys. 7 (18) (2005) 3297–3305.

[19] D.A. Patazis, X.Y. Chen, C.R. Landis, F. Neese, All-electron scalar relativistic basis sets for third-row transition metal atoms, J. Chem. Theory Comput. 4 (6) (2008) 908–919.

[20] R. Izsák, F. Neese, An overlap fitted chain of spheres exchange method, J. Chem. Phys. 135 (14) (2011).

[21] F. Neese, F. Wennmohs, A. Hansen, U.E. Becker, Approximate and parallel hartree-fock and hybrid DFT calculations. a 'chain-of-spheres' algorithm for the hartree-fock exchange, Chem. Phys. 356 (1–3) (2009) 98–109.

[22] V. Barone, M. Cossi, Quantum calculation of molecular energies and energy gradients in solution by a conductor solvent model, J. Phys. Chem. A 102 (11) (1998) 1995–2001.

[23] P. Pulay, Convergence acceleration of iterative sequences. the case of SCF iteration, Chem. Phys. Lett. 73 (2) (1980) 393–398.

[24] P. Pulay, Improved SCF convergence acceleration, J. Comput. Chem. 3 (4) (1982) 556–560.

[25] Molekel, Advanced Interactive 3D-Graphics for Molecular Sciences, Swiss National Supercomputing Centre. https://ugovaretto.github.io/molekel/ (accessed August 2023).

[26] K.N. Campbell, E.E. Young, The Addition of Hydrogen to Multiple Carbon-Carbon Bonds. IV. The Electrolytic Reduction of Alkyl and Aryl Acetylenes1, J. Am. Chem. Soc. 65 (5) (1943) 965–967.